Hindawi
Advances in Civil Engineering
Volume 2023, Article ID 6538496, 10 pages
https://doi.org/10.1155/2023/6538496

Research Article

Mechanical Property of Lateral Piles for Pile Composite Foundation Loaded by Model Test

Chen-xi Feng,[1] **Hang Yuan**,[2] **De-quan Zhou**,[3] **Peng Du**,[3] **Chuang-ye Wang**,[3] **Qiu-ling Yang**,[1] **Fei Pang**,[1] **Min Jing**,[1] **and Hui-xian Yu**[4]

[1]*School of Civil Engineering, Nanyang Institute of Technology, Nanyang, China*
[2]*China Construction Third Engineering Bureau Group Co., Ltd., Wuhan, China*
[3]*School of Civil Engineering, Changsha University of Science and Technology, Changsha, China*
[4]*School of Civil Engineering, Henan University of Technology, Zhengzhou, China*

Correspondence should be addressed to Chen-xi Feng; fengchenxi199011@163.com

Received 18 August 2022; Revised 7 December 2022; Accepted 29 December 2022; Published 25 April 2023

Academic Editor: Yi Zhang

Copyright © 2023 Chen-xi Feng et al. This is an open access article distributed under the Creative Commons Attribution License, which permits unrestricted use, distribution, and reproduction in any medium, provided the original work is properly cited.

Under vertical load, the composite foundation may be damaged due to insufficient lateral restraint capacity. If the lateral restraint pile is added to the edge of the composite foundation, the lateral stability can be effectively enhanced. This new reinforcement scheme is called a combined composite foundation. For the combined composite foundation, the lateral restraint piles will bear a certain force when the composite foundation is loaded, and the force may cause the piles horizontal displacement, instability, or even failure. After preload on the composite foundation, the mechanical behavior of lateral restraint piles will be more sophisticated. To study the mechanical behavior of lateral restraint piles under such condition, a laboratory model test was conducted. The results are suggested as follows: Axial force distribution curves tend to be "S" shape with two peak values at the upper and lower parts, respectively. The negative axial force is distributed at the upper part, and the positive axial force is distributed at the lower part. The bending moment and lateral soil pressure distribution of piles appear with the regularity of "increase-decrease" along the depth. Such a phenomenon is associated with the expansion of a potential slip surface. In accordance with the relative location of the potential slide surface and the piles, the lateral restraint piles can fall into three sections. Different sections get different stresses. The reinforcement scopes have an impact on the stress of different lateral restraint piles. With the increase of the reinforcement scope, the axial force, soil pressure, and bending moment show the regularity of increase. The values of axial force, the lateral soil pressure, and the bending moment increase with load growth and become stable when the load is larger than 60 kN. This is associated with the piles in the composite foundation, which verifies the reinforcement effect to prevent the soil slide and the foundation deformation.

1. Introduction

The traditional composite foundation can enhance the bearing capacity of foundation effectively, whereas the stability is fewer improved. To improve the bearing capacity and enhance the stability using the composite foundation, a new combination type of composite foundation is formed [1]. As in a traditional composite foundation, loose material piles or flexible piles (rigid pile) are set in the foundation to control vertical deformation (bearing capacity). Besides, high stiffness piles (laterally constraint pile) are set at the outer side of the foundation to control lateral deformation (stability). It is found in practice [2] that lateral restraint pile can significantly reduce the damage of composite foundation. Moreover, this pile has aroused great concern in the engineering field [3]. There has been a lot of research result on the working performance of composite foundation [1, 4] and lateral restraint pile [5–8] under the load. However, rare research studies were made on the working mechanism of this combined composite foundation. Under the load, the composite foundation generates settlement, and the laterally constraint piles will bear lateral earth pressure, skin friction,

and a bending moment [9–13]. The stress state of a lateral restraint pile is impacted by its length and stiffness, the value of the load, and the distance between the pile and load boundary [14–19].

The previous research studies primarily aimed at the mechanical property of lateral restraint pile under the condition of loading on the homogeneous foundation nearby. Moreover, the research methods primarily depend on the finite element analysis and theoretical analysis. Fewer laboratory and field experiments were performed.

For practical engineering, preload is commonly used to improve the bearing capacity of foundation. After preload on the combined composite foundation, its stress properties will be more sophisticated. It is not clear of the mechanical property of the lateral restraint pile under such condition. It to some extent limited the application of the "lateral restraint pile-composite foundation." In this paper, a model test is performed to study the engineering property of lateral restraint pile under the condition of load on the composite foundation nearby.

2. Model Test

This experiment was performed in a container with the internal dimension of 2500 mm × 1500 mm × 1500 mm ($l \times w \times h$). The arrangement of the lateral constrained piles (end bearing pile) and the composite foundation piles (friction pile) of the test are shown in Figure 1. The size of the test pile refers to the pile with the diameter of 1 m and the length of 24 m in the actual engineering. The parameters of model piles are summarized in Table 1. Lateral restraint piles are manufactured by cement mortar with the length of 1200 mm and the side length of 50 mm. The distance of pile B and A is 10 cm, 2 times of the pile side length. The distance of pile C and A is 20 cm, 4 times of the pile side length.

The model piles were manufactured in advance and placed in cement maintainer for 1 month. The strain gauge (Type: $B * 120–80AA$. Resistance value: 120.8 + 0.5 Ω. Gate length * width of the gate: 80 mm × 3 mm. The sensitive coefficient: 2.06) was pasted using the groove method [20] symmetrically on both sides of the piles. The distance of strain gauges from the top of piles are 40, 150, 260, 370, 480, 590, 700, 810, and 920 (mm), respectively. The elastic modulus of model piles is obtained by simply supported beam method. The earth pressure box (Dandong Sanda test instrument factory production, Model: DYB-2, Range: 0.1 MPa) was fixed using double sides adhesive on the surface of pile A. The distance of pressure boxes from the top of the pile are 0, 110, 220, 330, 440, 550, 660, 770, 880, and 990 (mm), respectively.

Model soil makes up of red clay and sand by a certain ratio, with the density of 1.26 g/cm^3, the moisture content of 2.5%, the maximum particle diameter of 5 mm, the uneven coefficient of 5.36, and the curvature coefficient of 1.39. As the model soil aggregate gradation curve is shown in Figure 2, the $D10$ is 0.11 mm, the $D30$ is 0.3 mm, the $D60$ is 0.59 mm, the Cu is 5.36 mm, and the Cc is 1.39 mm. The model soil is well graded. Before the test, the loading system is employed to process a cycle of load on the system of "lateral restraint pile-pile composite foundation" to achieve the preloading work. The largest preloading load is 120 kN. The test follows the specification of technical code for ground treatment of buildings (JGJ 79-2012). The process of test loading starts from 0 to 130 kN, and specifically, every load level is 10 kN. The information of the strain and the soil pressure box is gathered using the TDS-530 (with 130 channels) and the corresponding computer software.

3. Test Results

3.1. Axial Force Distribution of Piles. The strain generated by the resistance strain gauge is the same as that of the model pile. The pile shaft force is calculated (pressure stress is positive) in accordance with the strain value received by TDS-530 and the pile body elastic modulus obtained by calibration.

Figure 3 shows the variation curves of axial force N along with the distance z for the lateral restraint pile A, B, and C. The following is suggested from Figure 3:

(1) Under the load again, the axial force distribution curves of lateral restraint piles are shaped as an "S." The neutral point is positioned at 0.4 L under the ground surface. The negative axial force is distributed above the neutral point, while the positive axial force is distributed below the neutral point. There exists a maximum value of negative axial force at the upper part and another maximum value of positive axial force at the lower part. This phenomenon is similar to that the axial force characteristic of row piles subjected to the surcharge nearby [15]. For lateral restraint piles, the position of the negative maximum axial force value occurs at 0.15 L under the ground surface. And the position of the maximum positive axial force value occurs at 0.8 L-0.9 L under the ground surface. The maximum positive axial force value is bigger than the maximum negative axial force absolute value. At the initial phase of load, the axial forces of piles get rapid increase. Since the load is bigger than 60 kN, the rates of increase tend to be slow.

The above-mentioned phenomenon is associated with the soil in the foundation slide and creates pressure and friction on the lateral restraint piles. Figure 4 shows that there exists compressed triangle region in the upper part of the foundation. The soil in the compressed triangle region gets subsidence and squeezes the soil nearby. The soil nearby is slid or get sliding trend along the potential slide surface. The lateral restraint piles located in the sliding zone of soil and suffer acting force from the sliding soil.

In accordance with the relative location of the potential slide surface and the piles, the lateral restraint piles can be divided into three sections from top to bottom: the tension-bending section (T-B section), the bending-shear section (B-S section), and the compression-bending section (P-B section). The soil at the side of the T-B section slides toward tilt up. It

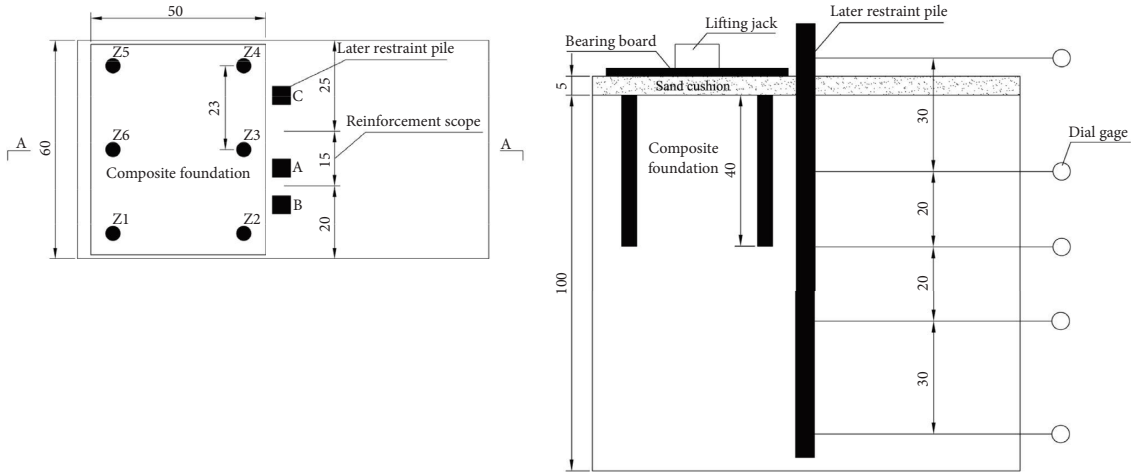

(a) (b)

Figure 1: Arrangements of the test. (a) Design of layout plan (unit: cm). (b) Sectional drawing of "*A*-*A*" (unit: cm).

Table 1: Parameters of model piles.

Pile numbers	Diameter or length (*D*/mm)	Length (*L*/mm)	Section shape	Elastic modulus (*E*/GPa)	Materials and pile types
A, *B*, *C*	50	1 200	Square	16.55	Cement mortar and end bearing pile
*Z*1, *Z*4	40	800	Circular	6.91	PVC tube filling Cement mortar and friction pile
*Z*2, *Z*5	40	800	Circular	6.91	
*Z*3, *Z*6	40	400	Circular	6.91	

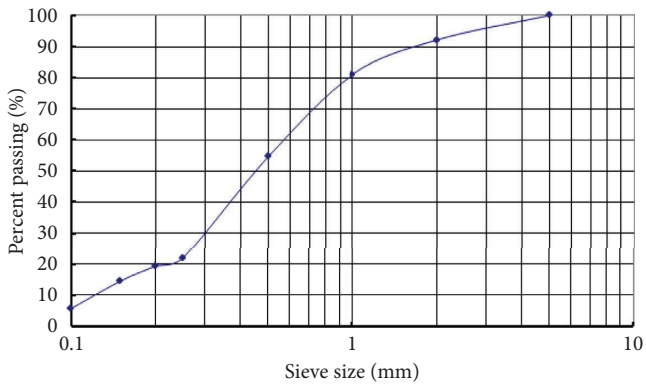

Figure 2: Grain-size distribution curve of model soil.

produces an upward friction force and horizontal pressure which make the pile section get positive axial force and bending moment. The soil at the side of *B*-*S* section slides toward the horizontal. It produces horizontal pressure, which makes the pile section get bending moment and shear force. The soil at the side of *P*-*B* section slides toward tilt down. It produces downward friction force and horizontal pressure which make the pile section get negative axial force and bending moment.

(2) In the experiment, the distance between the piles was defined the reinforcement scope of the pile. It can obtain the reinforcement scope of different lateral restraint piles from the plane position of Figure 1 and is shown in Table 2. Lateral restraint piles with different reinforcement scopes get different axial forces. Figure 5 shows the variation curves of maximum axial force values change with the reinforcement scopes under the load of 130 kN. In Figure 5, positive maximum axial force values show the regularity of increase as the growth of reinforcement scope. The negative maximum axial force values change slightly with the increase of the reinforcement scope.

Lateral restraint piles are located in the potential slide zone of the foundation and provide a constraint effect for the sliding soil. With the increase of the reinforcement scopes, the lateral restraint piles reinforce larger sliding soil and suffer larger force. The soil at the side of the upper section gives less force to the piles. So, the change of the reinforcement scope has little influence on the axial force.

3.2. Lateral Soil Pressure Distribution of Piles. In accordance with the strain values received by TDS-530 and the calibration equation of the pressure box, the values of soil pressure on the pile are calculated.

Figure 6 shows the soil pressure distribution curves of lateral restraint piles *A* under the load on the pile composite foundation again. It is observed as follows:

Before the load applied on the pile composite foundation again (the load is 0 kN), there still exists the lateral soil

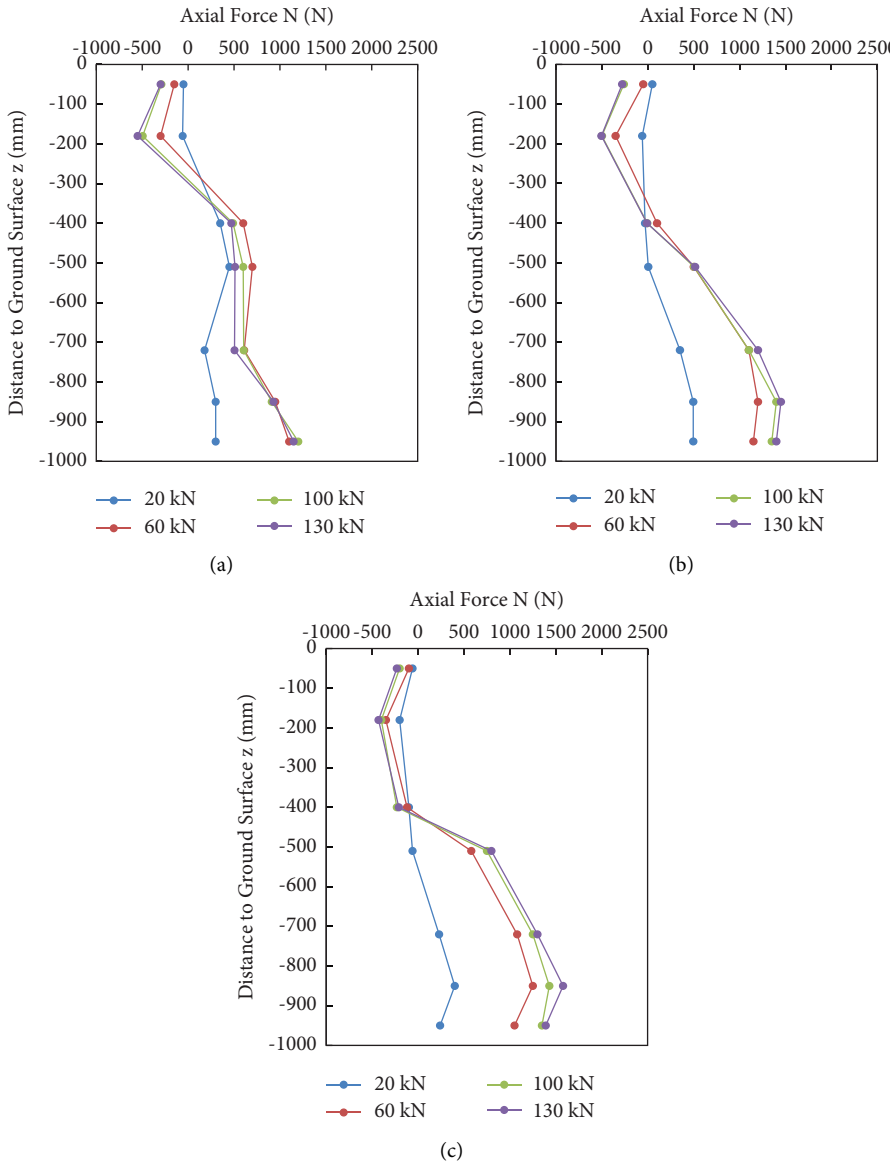

Figure 3: Axial force distribution curves. (a) Pile *A*. (b) Pile *B*. (c) Pile *C*.

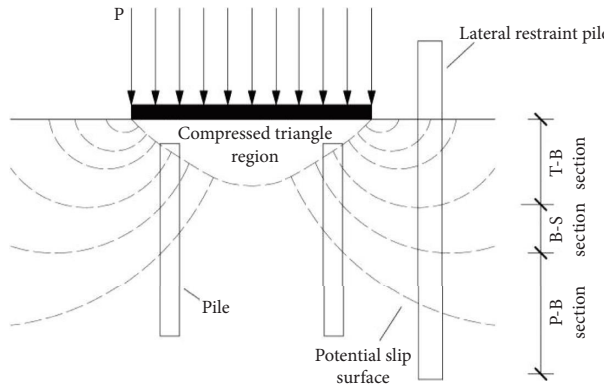

Figure 4: Stress state sections.

Table 2: Reinforcement scopes of lateral restraint piles.

Pile number	*A*	*B*	*C*
Reinforcement scope *S* (cm)	15	20	25

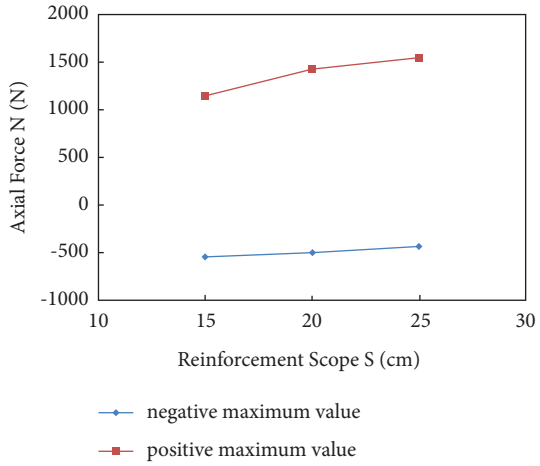

Figure 5: Regularity of maximum axial force values change with reinforcement scopes.

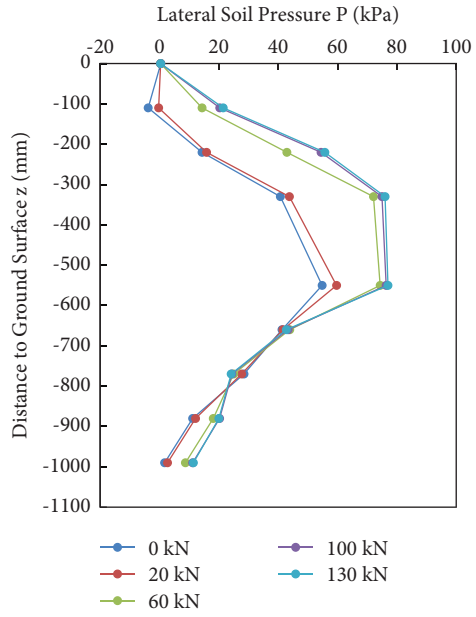

Figure 6: Soil pressure distribution curves.

pressure on the lateral restraint pile. It appears that the soil stress in the composite foundation cannot be the dissipation after the first unloading. With load growth, the pressure *P* growth less in the *T*-*B* section and the *P*-*B* section, whereas it gets a large increase in the *B*-*S* section. Under different loads, the soil pressure *P* shows the regularity of "increase-decrease" from top to bottom. There exists a maximum value located at *B*-*S* section.

Figure 7 shows the stress condition of different sections. The direction of the force of the pile is toward the tangent line of the potential slide surface. For the *T*-*B* section, the direction of the tangential force is toward tilt up. The tangential force can be decomposed into an upward vertical component force as well as a horizontal component force. The vertical component force produces frictional resistance. And the horizontal component force produces horizontal soil pressure. The horizontal component force varies with the tilt angle of the tangential force. In the *T*-*B* section, the tilt angle decreases from top to bottom, and the component force increases. In the *B*-*S* section, the direction of the force on the pile is nearly horizontal. Moreover, the soil pressure obtains the maximum value at the middle of the section. In the *P*-*B* section, the direction of the tangential force is toward tilt down. The tangential force can be decomposed into a downward vertical component force and the horizontal component force. The vertical component force produces frictional resistance. Furthermore, the horizontal component force produces horizontal soil pressure. In the *P*-*B* section, the tilt angle increases from top to bottom, and the component force decreases. It is verified that the *B*-*S* section is the major section to control the soil pressure of piles.

3.3. Bending Moment Distribution of Piles. Figure 8 shows the bending moment distribution curves of lateral restraint piles *A*, *B*, and *C* under the load on the pile composite foundation again.

The following can be observed:

(1) For lateral restraint piles, the bending moments appear with the regularity of "increase-decrease" from up to bottom along the depth *z*. It is similar to the variation of the lateral soil pressure. And for different piles, there exist maximum values on *B*-*S* sections. The position of the maximum value located at 0.37 L under the ground surface. The bending moments get little values on the *T*-*B* section and the *P*-*B* section. And they increase less as the load growth. For *B*-*S* section, the bending moments get large values. And they increase rapidly as load increase. At the initial phase of load, the bending moments of piles increase rapidly as the increase of load. When the load is large (60 kN), the bending moment change little with the increase of load.

The lateral soil pressure shows the regularity of "increase-decrease" from up to bottom along the depth *z* and gets maximum value at the middle of *B*-*S* section. The bending moment values primarily depend on the lateral soil pressure on the pile. Therefore, the *B*-*S* section suffers a larger bending moment, and this section is the major section to control bending failure.

(2) The reinforcement scope has a large impact on the bending moment of piles. Under the same load, the pile *C* get the largest maximum bending moment value, the pile *B* is second, and the pile *A* is the least. In accordance with the different reinforcement scopes of piles, the variation curve of maximum bending moment values change with reinforcement scope is shown in Figure 9. This figure shows that the

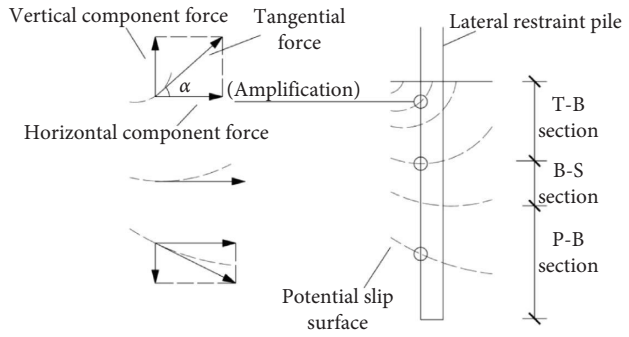

Figure 7: Stress state of sections.

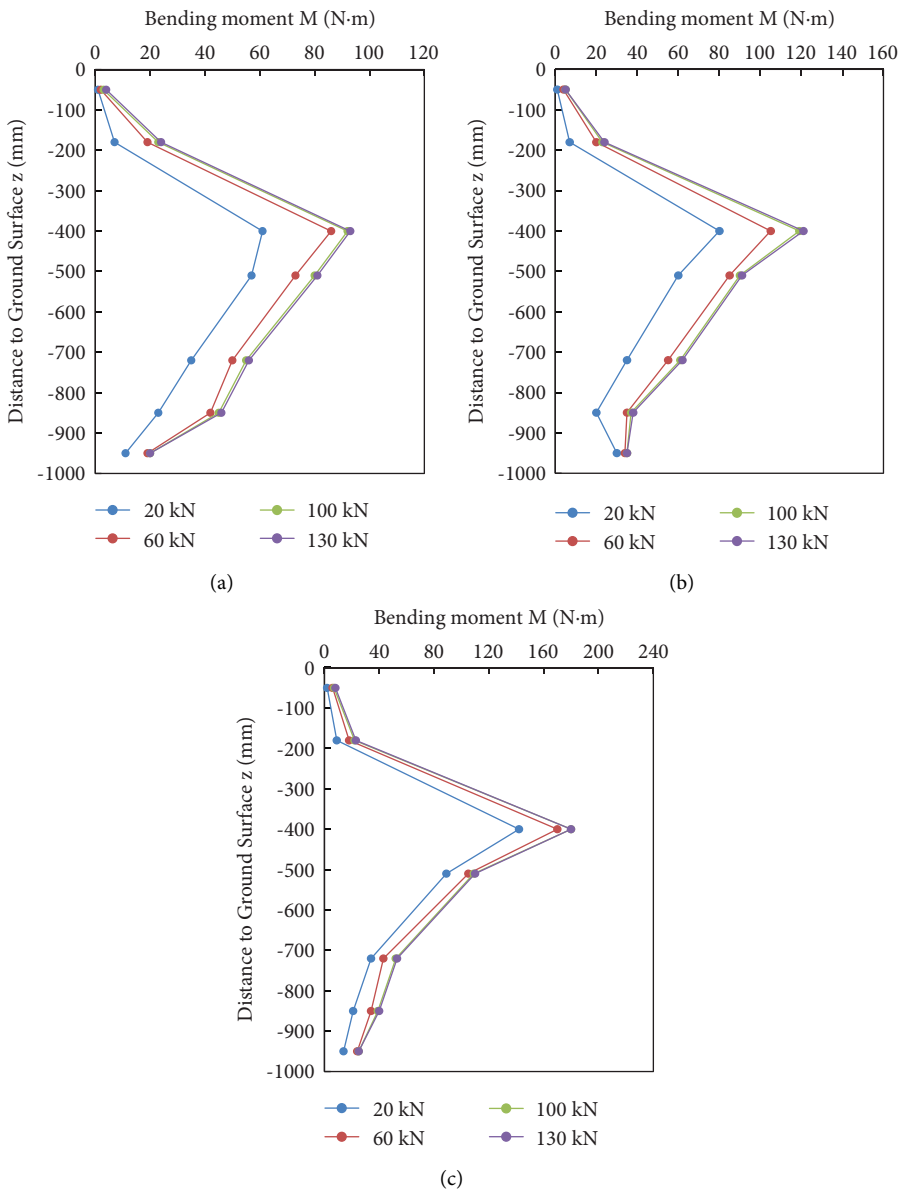

Figure 8: Bending moment distribution curves. (a) Pile *A*. (b) Pile *B*. (c) Pile *C*.

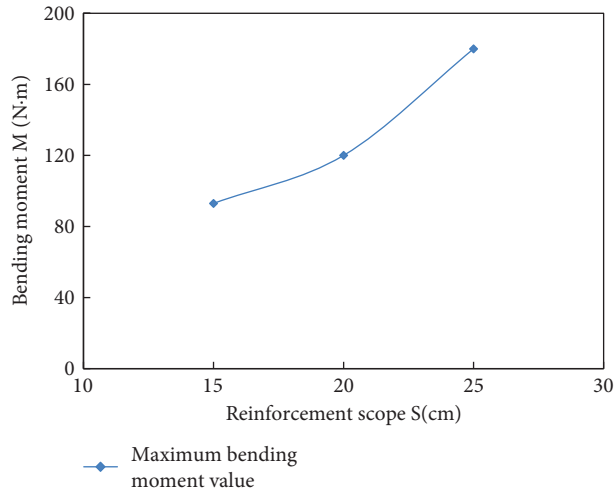

Figure 9: Regularity of maximum bending moment values change with reinforcement scopes.

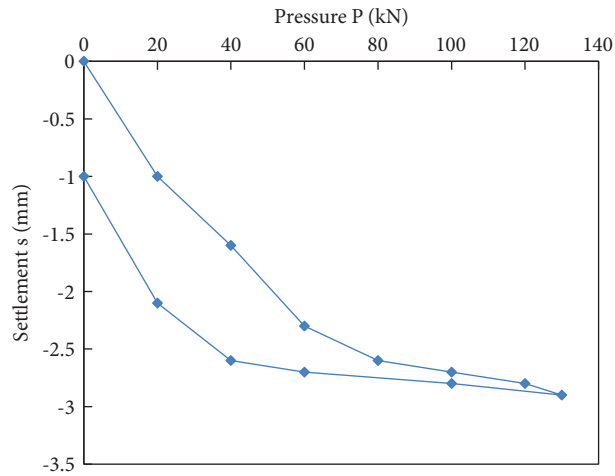

Figure 10: *P-S* curve of composite foundation.

maximum bending moment values increase with the increase of the reinforcement scope. It is suggested that with the increase of the reinforcement scope, the lateral restraint pile reinforces more sliding soil, suffers larger lateral soil pressure, and gets larger bending moment. And with the increase of the reinforcement scope, the growth rate of bending moment increase. Thus, with the increase of the reinforcement scope, the bending moment of piles increases rapidly. The pile is easy to get bending failure.

3.4. Deformation of Composite Foundation and Effect on Piles. Figure 10 is the *P-S* curve of the composite foundation under the load again. In the process of load, the settlement of the composite foundation increase as the load growth. When the load is larger than 60 kN, the settlement becomes gradually stable. In the process of unloading, the settlements change little when the load is larger than 40 kN. The settlement decreases rapidly when the load is smaller than 40 kN. The largest settlement of the foundation is 2.9 mm, and at last the total settlement is 1 mm after unloading. It verifies that the process of preloading eliminates most of the inelastic deformation already. In this exit, the inelastic deformation is 1 mm, and the elastic deformation is 1.9 mm.

Because of preloading on the foundation, the foundation primarily gets elastic deformation under 60 kN. The deformation of the foundation is primarily through the deformation of soil grain. The composite foundation supports the load as a whole. Piles in composite foundation do not have the reinforcement effect. When the load is larger than 60 kN, the soil in the foundation shows both the elastic deformation and the inelastic deformation. Soil and piles generate relative slip. Piles in composite foundation prove the reinforcement effect to prevent the soil slide and the foundation deformation.

Figure 11 shows the variation curve of the maximum axial force value, the maximum bending moment value, and the maximum soil pressure value change with the load, respectively. With the increase of the load, the values all

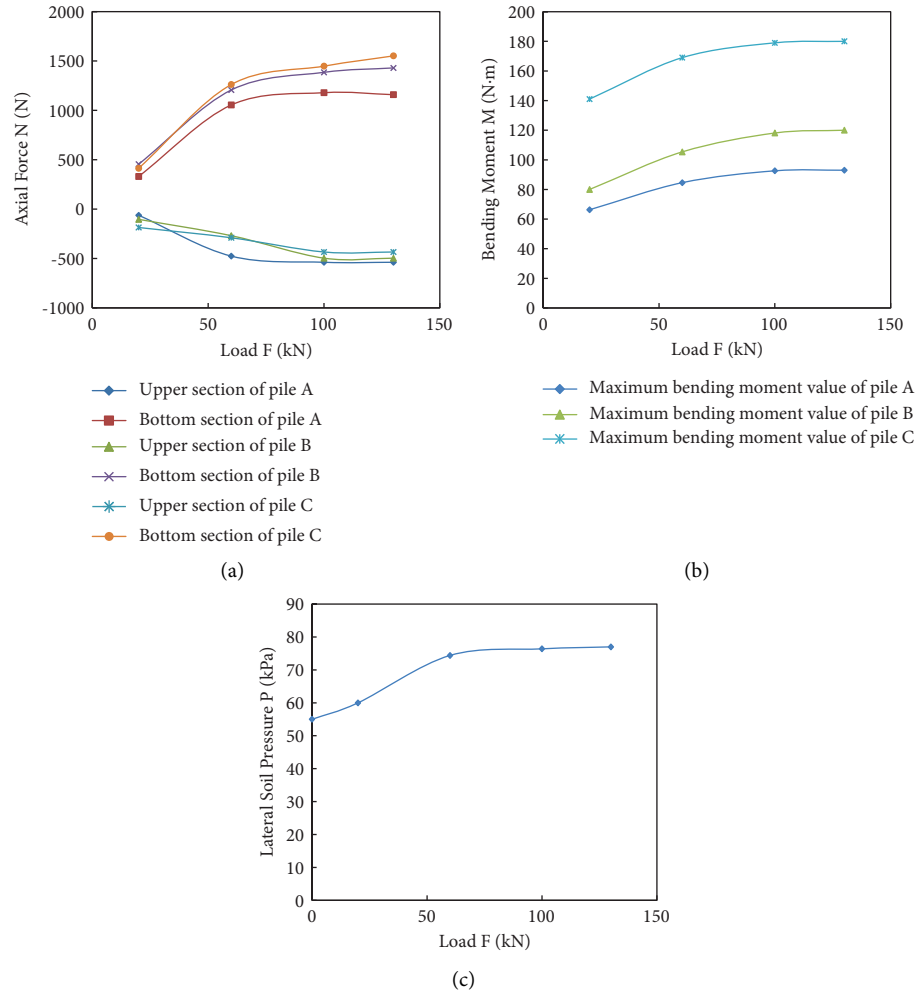

Figure 11: Maximum value variation curves. (a) Maximum axial force value variation curves. (b) Maximum bending moment value variation curves. (c) Maximum lateral pressure value variation curve.

show the trend of increase. When the load is less than 60 kN, the values increase rapidly. Since the load is larger than 60 kN, the values become stable. Analysis suggests that after preloading, the soil in the foundation is void less. The soil pressure transmits to the lateral restraint piles rapidly. Lateral restraint piles suffer vertical and horizontal force, and the force increase with the increase of load. When the load is larger than 60 kN, the piles in the composite foundation provide reinforcement effect, which prevents the soil pressure transmits to the lateral restraint piles.

4. Conclusion

Adding lateral restraint pile at the edge of composite foundation can effectively enhance the lateral stability of composite foundation. This paper studies the mechanical behavior of the lateral restraint pile under loading, with the following conclusions:

(1) Under the load again, there exist compressed triangle region in the upper part of the foundation. The soil nearby is slid or get sliding trend along the potential slide surface. In accordance with the relative location of the potential slide surface and the piles, the lateral restraint piles can be divided into three sections from top to bottom: the tension-bending section (*T-B* section), the bending-shear section (*B-S* section), and compression-bending section (*P-B* section). Different sections show different stresses. The *T-B* section suffers the soil pressure of the direction for tilt up, producing upward friction force and horizontal pressure. The *B-S* section suffers horizontal pressure. The *P-B* section suffers the soil pressure of the direction for tile down, producing downward friction force and horizontal pressure.

(2) For different piles, the axial force distribution curves of lateral restraint piles are in "*S*" shape. The neutral point is positioned at 0.4 L under the ground surface. The negative axial force is distributed above the neutral point, while the positive axial force is distributed under the neutral point. There exists a maximum value of negative axial force at the upper part and another maximum value of positive axial force at the lower part. Under different loads, the soil pressure *P* shows the regularity of "increase-

decrease" from top to bottom. There exists a maximum value located at *T-P* section. Similar to the variation of the lateral soil pressure, the bending moments appear the regularity of "increase-decrease" from up to bottom along the depth *z*. And the position of the maximum value is located at 0.37 L under the ground surface. This phenomenon is associated with the relative location of the potential slide surface and the piles.

(3) The reinforcement scopes have an impact on the stress of different lateral restraint piles. With the increase of the reinforcement scope, the axial force, the soil pressure, and the bending moment show the regularity of an increase. It is suggested that with the increase of the reinforcement scope, the lateral restraint pile reinforces more sliding soil, suffers larger lateral soil pressure, and gets larger force. And with the increase of the reinforcement scope, the growth rate of the bending moment increases. Thus, with the increase of the reinforcement scope, the bending moment of piles increases rapidly. The pile is easy to get bending failure.

(4) The process of preloading eliminates most of the inelastic deformation of the foundation. Under 60 kN, the foundation primarily shows the elastic deformation. The deformation of the foundation primarily results from the deformation of soil grain. As a whole, the composite foundation supports the load. Besides, the soil pressure transmits to the lateral restraint piles directly. The values of axial force, lateral soil pressure, and bending moment increase rapidly with the growth of the load. Since the load is larger than 60 kN, the soil in foundation exist inelastic deformation, and the soil grain slide. Soil and piles generate relative slip. Piles in composite foundation prove the reinforcement effect to prevent the soil slide and the foundation deformation. The values of axial force, lateral soil pressure, and bending moment become stable.

Data Availability

The data that support the findings of this study are available from the corresponding author upon reasonable request.

Conflicts of Interest

The authors declare that they have no conflicts of interest.

Acknowledgments

This work was financially supported by the Doctoral Research Startup Fund Project of Nanyang Institute of Technology (NGBJ-2022-19), which is greatly appreciated.

References

[1] D. Q. Zhou, C. Yan, and W. H. Luo, "An experimental study of deformation of laterally constraint pile of composite pile foundation during repetitive loading/unloading," *Rock and Soil Mechanics*, vol. 36, no. 10, pp. 2780–2786, 2015.

[2] Y. C. Yao, Y. X. Wei, and B. Y. Yuan, "Exploration on the deformation and control of embankment constructed on slope foundation for high- speed railways," *Journal of Railway Engineering Society*, vol. 5, pp. 16–21, 2014.

[3] L. Chen and H. G. Poulos, "Analysis of pile-soil interaction under lateral loading using infinite and finite elements," *Computers and Geotechnics*, vol. 15, no. 4, pp. 189–220, 1993.

[4] H. L. Liu and M. H. Zhao, "Review of ground improvement technical and its application in China," *China Civil Engineering Journal*, vol. 49, no. 1, pp. 96–115, 2016.

[5] M. F. Bransby and S. M. Springman, "3-D finite element modelling of pile groups adjacent to surcharge loads," *Computers and Geotechnics*, vol. 19, no. 4, pp. 301–324, 1996.

[6] D. P. Stewart, R. J. Jewell, and M. F. Randolph, "Design of piled bridge abutments on soft clay for loading from lateral soil movements," *Géotechnique*, vol. 44, no. 2, pp. 277–296, 1994.

[7] H. G. Poulos, L. T. Chen, and T. S. Hull, "Model tests on single piles subjected to lateral soil movement," *Soils and Foundations*, vol. 35, no. 4, pp. 85–92, 1995.

[8] K. N. Kim, S. H. Lee, K. S. Kim, C. K. Chung, M. M. Kim, and H. S. Lee, "Optimal pile arrangement for minimizing differential settlements in piled raft foundations," *Computers and Geotechnics*, vol. 28, no. 4, pp. 235–253, 2001.

[9] M. Y. Fattah, R. R. Al-Omari, and S. H. Fadhil, "Load sharing and behavior of single pile embedded in unsaturated swelling soil," *European Journal of Environmental and Civil Engineering*, vol. 24, no. 12, pp. 1967–1992, 2020.

[10] S. Fadhil, R. Al-Omari, and M. Y. Fattah, "Distribution of axial force and shear stress along a compression pile embedded in saturated and unsaturated swelling soil," in *Proceedings of the 20th International Conference on Soil Mechanics and Geotechnical Engineering– Rahman and Jaksa*, pp. 3271–3276, Australian Geomechanics Society, Sydney, Australia, June 2022.

[11] S. H. Fadhil, R. R. Al-Omari, and M. Y. Fattah, "Measuring pile shaft and tip capacities of a single pile embedded in saturated and unsaturated expansive clayey soil," *IOP Conference Series: Materials Science and Engineering*, vol. 737, no. 1, Article ID 012086, 2020.

[12] R. R. Al-Omari, M. Y. Fattah, and S. H. Fadhil, "Adhesion factor of piles embedded in unsaturated swelling soil," in *Proceedings of the 19th International Conference on Soil Mechanics and Geotechnical Engineering*, pp. 2703–2706, ICSMGE, Souel Korea, July 2021.

[13] M. Y. Fattah, R. R. Al-Omari, and A. M. Kallawi, "Model studies on load sharing for shaft and tip of pile groups in saturated and unsaturated soils," *Geotechnical and Geological Engineering*, vol. 38, no. 4, pp. 4227–4242, 2020.

[14] B. B. Broms, "Can lime/cement columns be used in Singapore and Southeast Asia?" in *3rd GRC Lecture*,p. 214, Singapore, 1999.

[15] M. Ashour and H. Ardalan, "Analysis of pile stabilized slopes based on soil–pile interaction," *Computers and Geotechnics*, vol. 39, no. 1, pp. 85–97, 2012.

[16] Y. M. Tu and J. J. Wang, "Study on negative friction characteristic of row piles subjected to surcharge nearby," *Rock and Soil Mechanics*, vol. 28, no. 12, pp. 2652–2656, 2007.

[17] Y. M. Tu and Y. N. Yu, "3D finite element analysis of bending property of passive row piles," *Rock and Soil Mechanics*, vol. 29, no. 2, pp. 342–346, 2008.

[18] Y. Xie, S. H. Zhang, and D. Q. Zhou, "Experimental study of mechanical behavior of passive loaded piles adjacent to piled foundation," *KSCE Journal of Civil Engineering*, vol. 22, no. 10, pp. 3818–3826, 2018.

[19] D. Q. Zhou, H. L. Liu, and K. N. Zhang, "Experimental comparison study on behavior of three and four-element composite foundation," *Journal of Building Structures*, vol. 25, no. 5, pp. 124–129, 2004.

[20] D. Q. Zhou, K. Chen, M. H. Zhao, and L. Chen, "Technique and application of strain gauge pasted on low strength model pile in indoor model experiment," *Journal of Experimental Mechanics*, vol. 24, no. 6, pp. 558–562, 2009.